Enhanced reaching law for improved response in sliding mode control of PMSM motors with fuzzy logic integration

Khanh Quoc Truong, Son Huynh, Dung Hoang Vo, Minh Duc Pham
Power Electronics Research Laboratory, Faculty of Electrical and Electronics Engineering,
Ho Chi Minh City University of Technology (HCMUT), Ho Chi Minh City, Vietnam
Vietnam National University, Linh Trung Ward, Thu Duc City, Ho Chi Minh City, Vietnam

Article Info	ABSTRACT
	The rising demand for high-performance permanent magnet synchronous motors (PMSMs) is responsible for the development of PMSM speed control. Although the proportional-integral controller is often used in field-oriented control (FOC) for motor speed regulation, it has drawbacks like slow response and instability. This paper proposed an enhanced sliding mode controller with a modified sliding surface to achieve better speed control performance. In comparison to proportional-integral or PI controller, fuzzy logic controller, conventional sliding mode controller, the proposed control approach uses a reaching law that incorporates a fuzzy logic controller. A smoother and faster response time is targeted by the proposed approach compared to conventional sliding mode control. Practical small-scale PMSM experiments certify the effectiveness of our proposed enhanced sliding mode control. *This is an open access article under the [CC BY-SA](#) license.*

Corresponding Author:

Minh Duc Pham
Power Electronics Research Laboratory, Faculty of Electrical and Electronics Engineering
Ho Chi Minh City University of Technology (HCMUT)
268 Ly Thuong Kiet Street, District 10, Ho Chi Minh City, Vietnam
Email: pmduc@hcmut.edu.vn

1. INTRODUCTION

Permanent magnet synchronous motors (PMSMs) are now being widely used in many applications due to their high-power density, efficiency, and torque-to-current ratio. Their speed performance is significant, and they are critical in applications such as robotics, electric vehicles, and machine tools [1], [2]. In an excavator, for instance, suitable speed regulation enables the machine to move precisely and effectively perform excavation operations. It ensures that lifting and lowering heavy loads are done smoothly, increasing operational safety when used by cranes and elevators. Controlling the speed of a PMSM is important in electric vehicles (EVs) for acceleration, maintaining constant velocity, and effectively operating regenerative braking. In contrast, torque control is common in heavy industry applications such as excavators and product conveyor belts. The importance of speed control versus torque control varies significantly depending on application. In this research, we are particularly focused on designing a speed controller for PMSM motor in EV acceleration systems.

PMSMs are characterized by nonlinear and multi-variable dynamics influenced by flux linkage and direct-quadrature or DQ-axes inductances, which can vary during motor operation due to magnetic saturation. It is also difficult to produce both high accuracy and speed, as PMSMs exhibit strong nonlinearity due to the strong coupling between torque and speed in a mechanical model. To address the complex issues arising from the mechanical equation of PMSMs, the field-oriented control (FOC) technique emerged [3]-[5]. In the FOC technique, the motor control system is transformed into a synchronous reference frame, simplifying the control task by decoupling the torque and flux components.

The outer control loop is the speed control loop, responsible for generating the q-axis reference current. The inner control loop regulates the motor current using a proportional-integral (PI) controller within the DQ frame. This PI control loop effectively tracks the d and q components of the motor current references, ensuring precise control over torque and flux. To control the PMSM motor speed, the linear PI controller is employed to adjust the q current reference of the inner control loop for tracking motor speed [6]-[8]. Although PI speed control offers adequate control precision and robustness, it often falls short in terms of slow response and stability when confronted with disturbances such as load changes and variations in speed [9], [10]. Conventional studies on PMSM speed control using the PI controller specifically highlight significant challenges related to speed response and stability [11]-[13]. That is because speed regulation tends to be a linear calculation, but PMSM dynamics are non-linear. For this reason, more improved control methods are needed to improve the slow response problem and system stability.

Nonlinear control techniques have emerged as potential alternatives that can address the limitations of linear controllers [14]-[16]. Nonlinear control techniques such as adaptive control, predictive control, and sliding mode control have demonstrated the potential to improve the stability, precision, and robustness of PMSM motor control. Adaptive control can handle uncertainties by adjusting control parameters in real-time, but it needs accurate system parameters and may cause system instability [17]-[19]. However, on the other hand, predictive control involves predicting future system behavior which is able to achieve satisfactory performance but at high computational costs and sensitivity due to system mismatches [20]-[22]. Sliding mode control provides robustness in the presence of uncertainties and disturbances using discontinuous controls; however, it may introduce chattering problems [23]-[25]. The use of sliding mode control is important for stability reasons in the presence of disturbances and uncertainties.

Given the drawbacks of previous works, it requires an improved control law and reaching conditions for chattering attenuation along with speed response improvements. An enhanced sliding mode control is presented in this paper to improve control response and stability with reduced chattering. A sliding surface with the improved reaching law is added in this proposed control approach, which also includes fuzzy logic control integration. These modifications will allow the system state to arrive at the sliding surface as fast as possible and reduce chattering of control actions thanks to the adjustable sliding gain. Furthermore, the system is always stable with this defined reaching law. This control approach not only provides smoother dynamics but also obtain a shorter response time than the conventional sliding mode control. The control theory is verified by means of experimental results with a small-scale PMSM system.

2. FOC AND MATHEMATICAL MODEL OF PMSM
2.1. Principle of FOC algorithm
In permanent magnet synchronous motors, the stator current affects both the magnetic flux and the generated torque. Hence, field-oriented control was proposed to decouple flux and torque can be achieved by analyzing the instantaneous current into two components: One component aligned with the rotor magnetic field, called the direct axis (d), and the other perpendicular to the rotor magnetic field, called the quadrature axis (q) [26]. Field-oriented control is the basic idea of synthesizing sinusoidal inverter voltage to provide progressive speed control with optimal torque output. Maximum torque is reached when the angle between the magnetic fields of the stator and rotor becomes 90 degrees. The stator magnetic flux is aligned orthogonally to the rotor by forcing the d-axis current to 0 and properly adjusting the q-axis.

2.2. Coordination between speed controller and FOC
The block diagram of a conventional speed controller with FOC with speed controller is shown in Figure 1. In the figure, the control process begins with measuring the motor three-phase currents, which are then transformed through Clark and Park transformations to obtain currents along the independent d and q axes. Then, the current rotor speed is compared with the reference speed (ω_m^*) to generate a speed error signal ($x_1 = (\omega_m^* - \omega_m)$), which is fed into an outer speed controller to produce a reference current along the q-axis (i_q^*). In the inner control loop, two PI controllers are utilized to regulate the currents along the d and q axes, generating reference voltage signals along these axes independently (u_q, u_d). Following this, inverse Clark and Park transformations are applied to convert the voltage signals from the dq axes to three-phase voltage signals for the space vector pulse width modulation (SVPWM) block. The SVPWM is a modulation technique used to generate PWM signals for controlling the switching devices in an inverter [27]-[29].

2.3. Mathematical model of PMSM
To implement the FOC algorithm on a digital processor, a mathematical model of the motor is essential. Through the Clark and Park transformation, the mathematical model of the PMSM is transformed into the following mathematical representation in the DQ frame. Where U_d, U_q are d-axis and q-axis voltages,

i_d, i_q are d-axis and q-axis currents, L_d, L_q are d-axis and q-axis inductance, R_s is coil resistance, ω_e is the electrical speed of the rotor, ω_m is the mechanical angular speed of the rotor, and ψ_f is permanent magnet flux linkage. For the steady state, the differential terms can be disregarded since there are no variations in currents, the (1) can be simplified as (2).

$$\begin{cases} U_d = R_s i_d - \omega_e L_q i_q + L_d \frac{di_d}{dt} \\ U_q = R_s i_q + \omega_e (L_d i_d + \psi_f) + L_q \frac{di_q}{dt} \end{cases} \tag{1}$$

$$\begin{cases} U_d = R_s i_d - \omega_e L_q i_q \\ U_q = R_s i_q + \omega_e (L_d i_d + \psi_f) \end{cases} \tag{2}$$

The relationship between electromagnetic torque and the d and q-axis currents in the DQ reference frame is given by the (3):

$$\begin{cases} T_e = \frac{3}{2} p [\psi_f + (L_d - L_q) i_d] i_q \\ T_e - T_L = \frac{J}{p} \frac{d\omega_m}{dt} \end{cases} \tag{3}$$

where T_e is electromagnetic torque, T_L is load torque, p is number of the pole pairs, J is inertia moment. In the FOC algorithm, assuming the angle θ is accurately measured from the motor, to achieve the optimal torque, controlling the current $i_d = 0$ is necessary. Then, the dynamic equation of the PMSM motor is simplified as (4).

$$\begin{cases} T_e = \frac{3}{2} p \psi_f i_q \\ \frac{3}{2} p \psi_f i_q - T_L = \frac{J}{p} \frac{d\omega_m}{dt} \end{cases} \tag{4}$$

In (4), the relationship between the mechanical angular speed of the rotor ω_m and the controlled current on the quadrature axis (i_q) is determined. This relationship forms the fundamental equation for controlling the mechanical angular speed to generate the reference current i_q^*.
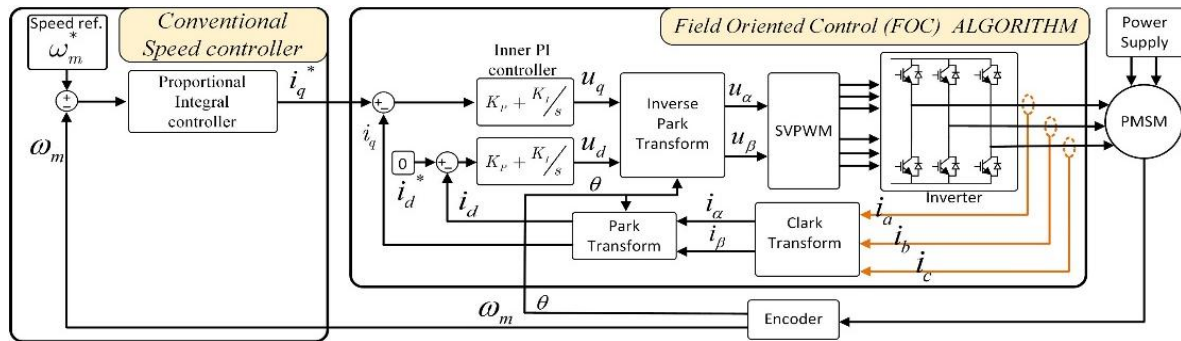

Figure 1. Block diagram of FOC with speed controller

3. STATE VARIABLES OF THE PMSM SPEED CONTROLLER AND CONVENTIONAL SLIDING MODE CONTROL

Sliding mode control ensures stability in uncertain and noisy conditions through discontinuous control laws. However, selecting an inappropriate sliding surface can lead to chattering problems, which are common issues in sliding control systems. Thus, designing a sliding mode control system with reduced chattering is crucial. This drives the research to develop an enhanced approach based on the challenges arising from conventional approaches.

3.1. Formulating the state variables of the PMSM speed controller

The system state variables of the speed controller are defined as (5). Where ω_m^* and ω_m are speed references and the instant speed of the PMSM motor. Derived from (5), $\dot{x}_2$ is derived as (6).

$$\begin{cases} x_1 = e = \omega_m^* - \omega_m \\ x_2 = \dot{e} = \frac{dx_1}{dt} = -\frac{d\omega_m}{dt} = -\frac{p}{J}\left(\frac{3}{2}p\psi_f i_q - T_L\right) \end{cases} \tag{5}$$

$$\dot{x}_2 = \ddot{e} = -\frac{d^2\omega_m}{dt^2} = -\frac{3p^2}{2J}\psi_f \frac{di_q}{dt} \tag{6}$$

For simplicity, we assign $\frac{3p^2}{2J}\psi_f$ and $\frac{di_q}{dt}$ in (6) as (7).

$$K = \frac{3p^2}{2J}\psi_f; U = \frac{di_q}{dt} \tag{7}$$

From (5) and (6), the state equation of the system can be expressed as (8).

$$\begin{bmatrix} \dot{x}_1 \\ \dot{x}_2 \end{bmatrix} = \begin{bmatrix} 0 & 1 \\ 0 & 0 \end{bmatrix}\begin{bmatrix} x_1 \\ x_2 \end{bmatrix} + \begin{bmatrix} 0 \\ -K \end{bmatrix} U \tag{8}$$

Once the system state variables are identified, the subsequent step involves selecting a representative sliding surface, typically as in (9).

$$s = x_2 + cx_1 \tag{9}$$

With the expression of the sliding surface, the value of the coefficient c is correlated with the asymptotic stability of the sliding mode and the convergence rate towards the sliding surface. Given the defined sliding surface, the reference current along the q-axis (i_q^*) can be determined from its expression (9) as in (10).

$$\dot{s} = \dot{x}_2 + c\dot{x}_1 = \dot{x}_2 + cx_2 \rightarrow \dot{x}_2 = \dot{s} - cx_2 = -K\frac{di_q^*}{dt} \rightarrow di_q^* = \frac{1}{K}(-\dot{s} + cx_2)dt \tag{10}$$

Taking the integral of both sides of (10), we obtain (11).

$$i_q^* = \frac{1}{K}\int(-\dot{s} + cx_2)dt \tag{11}$$

The expression for the reference current i_q^* in (11) forms the basis for developing the control algorithm for the speed controller. Through this expression, the dependency of the sliding surface convergence rate $\dot{s}$ on generating the reference current i_q^* can be observed, and designing the equation for $\dot{s}$ is crucial and directly impacts control performance. Assuming that the PMSM angle is accurately measured from the motor encoder, the motor speed ω_m is calculated, and this value is used to determine x_1 and x_2. Then, these state variables are used to determine the reference current i_q^*, as shown in (11).

3.2. The conventional reaching law method

The conventional reaching law method aims to ensure fast convergence of the system to the sliding surface while mitigating chattering and overshoot. The linear reaching law offers simplicity and ease of implementation. The conventional reaching law is design is given by (12). In the conventional reaching law method, the reaching time t_1 is defined as the time required for the states to approach the sliding surface, and it can be used to evaluate the controller performance. The reaching time t_1 can be calculated according to (12) as in (13).

$$\dot{s} = -\varepsilon\, sgn(s) \tag{12}$$

$$\dot{s} = \frac{ds}{dt} = -\varepsilon\, sgn(s) \rightarrow \int_0^{t_1} dt = \int_{S(0)}^0 \frac{1}{-\varepsilon\, sgn(s)} ds \rightarrow t_1 = \frac{S(0)}{\varepsilon} \tag{13}$$

Based on the above expression, it can be seen that the reaching time t_1 depends on the constant ε, and the initial state position of $S(0)$. To improve the time to reach the sliding surface t_1, the constant q is

introduced. The linear reaching law in the conventional method in [24] offers improvement in reaching time t_1, making it a popular choice in many control applications. The conventional reaching law is designed as in (14):

$$\dot{s} = -\varepsilon\, sgn(s) - qs \tag{14}$$

where ε, q are positive constants. Substituting (14) into (11), we have the following current reference as in (15).

$$i_q^* = \frac{1}{K} \int (\varepsilon\, sgn(s) + qs + cx_2)\, dt \tag{15}$$

From (15), it is necessary to consider the influences of constants ε and q in controlling the speed of PMSM. In particular, a larger value of constants ε and q results in a shorter approach time. However, this also leads to a sudden increase in motor speed, potentially causing it to slide out of the s surface and resulting in chattering. Furthermore, if the initial position $S(0)$ is further from the sliding surface, the approach time will significantly increase.

In sliding mode control, the chattering issue often occurs when the control system is operating near the boundary of the sliding surface, where small perturbations or uncertainties can cause the control signal to fluctuate rapidly between different values. This issue may lead to instability, degraded performance, and increased energy consumption. To analyze the chattering issue, $\dot{s}$ in the continuous domain is converted to the discrete domain. As real-time control is indispensable in practical control system implementations, control operations must be carried out within a discrete domain. From (14), the discrete expression of the conventional reaching law method as s approaches 0 is represented as in (16):

$$s(n+1) - s(n) = -\varepsilon T\, sgn(s(n)) \tag{16}$$

where T is the sampling time. Under the assumption that the system trajectory reaches the sliding-mode surface within a finite step, which implies that $s(n) = 0^+$ and $s(n) = 0^-$, the equation for the subsequent period can be derived with $s(n) = 0^+$ and $s(n) = 0^-$ as in (17).

$$s(n+1) = -\varepsilon T\,(when\, s(n) = 0^+); \quad s(n+1) = \varepsilon T\,(when\, s(n) = 0^-) \tag{17}$$

The width of the discrete sliding-mode band δ_1 is calculated between the boundary $s(n) = 0^+$ and $s(n) = 0^-$. Figure 2 shows the state trajectory of the conventional reaching law. It can be seen in Figure 2 that the width of the discrete sliding-mode band δ_1 in (18) causes the system to fail to reach the equilibrium point O and the state trajectory oscillating around the point O. This result leads to a significant chattering problem when increasing parameter ε to reduce the reaching time to the sliding surface.

$$\delta_1 = 2\varepsilon T \tag{18}$$
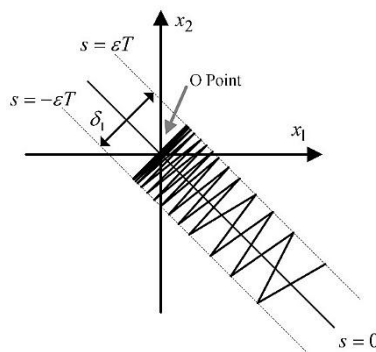

Figure 2. State trajectory of the conventional reaching law

4. PROPOSED ENHANCED REACHING LAW DESIGN WITH FUZZY LOGIC CONTROLLER
4.1. The basic idea of enhanced reaching law integrated with fuzzy logic controller

To effectively address the chattering issue and improve the system response, it is essential to establish two coefficients q and ε as variables that can change according to the state variable x_1 and the sliding surface

position s. This forms the basis for proposing enhanced reaching law design with fuzzy logic controller for adaptive adjusting of coefficients q and ε. Additionally, the gain $fuzzy(q)$ is adaptively adjusted using the proposed fuzzy logic controller. Hence the proposed reaching law is given by the (19):

$$\dot{s} = -\frac{\varepsilon|x_1|^a}{m|x_1|^a + ke^{-\zeta|s|}} sgn(s) - fuzzy(q)s \tag{19}$$

where $\varepsilon, m, a, k, \zeta$ are positive constants and $0 < m < 1$, $fuzzy(q)$ is the output of the fuzzy logic controller according to the input s and $\dot{s}$. The proposed reaching law is analyzed in two states: reaching the sliding mode surface and operating near the boundary of the sliding surface. For simplicity, the system is analyzed when the system state variable is positive.

In the reaching sliding mode surface state, the system state variable is located far away from the sliding surface, so that $ke^{-\zeta|s|} \approx 0$. Hence the (19) will converge to the (20).

$$\dot{s} \approx -\frac{\varepsilon}{m} sgn(s) - fuzzy(q)s \tag{20}$$

Compared to the conventional reaching law in (14), which the coefficient q is a fixed number, the proposed reaching law has the adaptive reaching gain $fuzzy(q)$. This fuzzy output is adaptively adjusted according to the input s and $\dot{s}$. Thanks to the adaptive adjustment of fuzzy output, the reaching time is improved with a high gain $fuzzy(q)$, and this variable is reduced when approaching the sliding mode surface.

In the boundary operation of the sliding surface state, the following condition is satisfied $s \to 0$, and the (19) will converge to the (21). The (21) depend on x_1, and its value is gradually reduced to 0 as x_1 moves to the origin. The proposed control law contributes to a smooth response when the system state x_1 near the sliding surface, which contribute to eliminate chattering issues. The combination of adaptive gains $fuzzy(q)$ in the reaching sliding mode surface state and $\frac{\varepsilon|x_1|^a}{m|x_1|^a + k}$ in the boundary operation of the sliding surface, the state contributes to the improved system response and chattering reduction. Figure 3 shows the block diagram of the proposed enhanced sliding mode control.

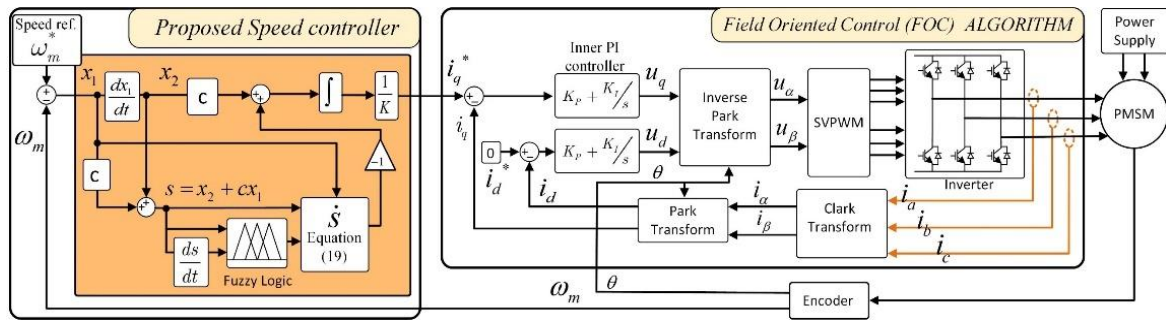$$\dot{s} \approx -\frac{\varepsilon|x_1|^a}{m|x_1|^a + k} sgn(s) \tag{21}$$

Figure 3. Block diagram of the proposed enhanced sliding mode control

4.2. The design of fuzzy(q) in fuzzy logic controller

The control variable $fuzzy(q)$ is the output of the fuzzy logic controller, allowing an adaptive tune according to the state variables x_1 and x_2. Based on the experience, the input coefficient of the state variables x_1 and x_2 range from [-10; 10], and the output $fuzzy(q)$ with gain ranges from 0 to 2000. The fuzzy set is defined as follows: $s = \{NB, NM, NS, ZE, PS, PM, PB\}$; $\dot{s} = \{NB, NM, NS, ZE, PS, PM, PB\}$, where negative big (NB), negative medium (NM), negative small (NS), zero (ZE), positive small (PS), positive medium (PM), and positive big (PB) represent different levels of input variables. The output $fuzzy(q) = \{S, MS, M, MB, B\}$, where small (S), medium small (MS), medium (M), medium big (MB), and big (B) represent different levels of output. The fuzzy rule table is provided in Table 1 and the relationship between s, $\dot{s}$, and the output $fuzzy(q)$ is shown in Figures 4(a)-4(c). By using the membership functions and fuzzy rule table, the coefficient q is adaptively adjusted according to the value of s and its derivatives. The 3D plot of q, s, ds/dt, and their relationship is shown in Figure 5. When s and its derivative have high values, which indicates the state

trajactory is located far from the sliding surface, the coefficient q is increased to enhance the reaching speed to the sliding surface. On the other hand, when the value s and its derivative are small, when means the state trajectory is near the sliding surface, the coefficient q is minimized to ensure that the state trajectory reaches the sliding surface without overshoot.

Table 1. The rule base of the fuzzy controller

s	$\dot{s}$						
	NB	NM	NS	ZE	PS	PM	PB
NB	B	MB	M	MS	M	MB	B
NM	MB	M	M	M	M	M	MB
NS	MB	M	MS	S	MS	M	MB
ZE	M	MS	S	S	S	MS	M
PS	MB	M	MS	S	MS	M	MB
PM	MB	M	M	M	M	M	MB
PB	B	MB	M	MS	M	MB	B

(a)

(b)

(c)
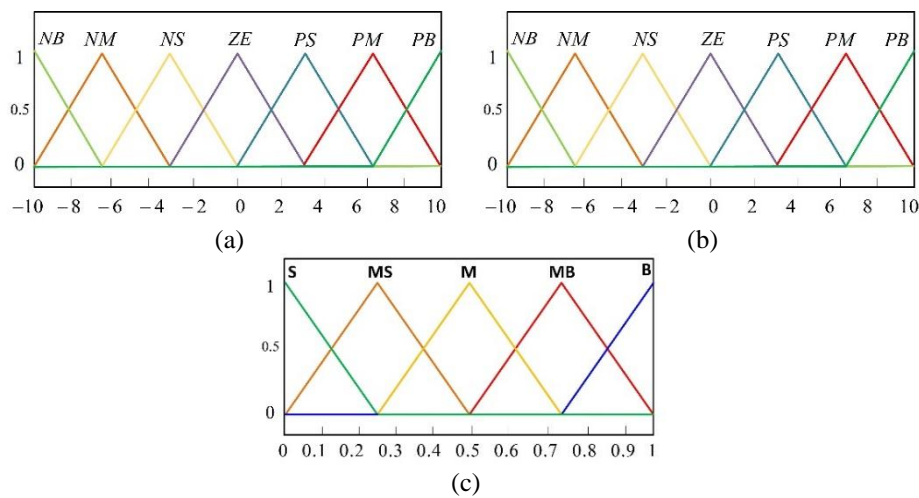
Figure 4. The membership function of the fuzzy controller for input s, $\dot{s}$, and $fuzzy(q)$:
(a) input s, (b) input $\dot{s}$, and (c) output $fuzzy(q)$
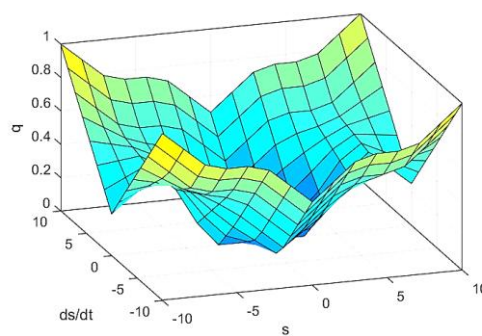
Figure 5. The fuzzy logic control surface

Substituting (19) into (11), reference current i_q^* is obtained as (22).

$$i_q^* = \frac{1}{K} \int \left(\frac{\varepsilon|x_1|^a}{m|x_1|^a + ke^{-\zeta|s|}} sgn(s) + fuzzy(q)s + cx_2 \right) dt \tag{22}$$

In the boundary operation of the sliding surface state, the sliding mode surface s approaches 0, and the proposed enhanced reaching law in (19) can be converted to the discrete-time domain as (23):

$$s(n+1) - s(n) = -\frac{\varepsilon T|x_1|^a}{m|x_1|^a + k} sgn(s(n)) \tag{23}$$

where T represents the sampling period. Under the assumption that the system's trajectory reaches the sliding-mode surface within a finite step, which implies that $s(n) = 0^+, s(n) = 0^-$, the equation for the subsequent period can be derived with $s(n) = 0^+$ and $s(n) = 0^-$ as in (24).

$$s(n+1) = -\frac{\varepsilon T|x_1|^a}{m|x_1|^a + k}(when s(n) = 0^+); \quad s(n+1) = \frac{\varepsilon T|x_1|^a}{m|x_1|^a + k}(when s(n) = 0^-) \tag{24}$$

The width of the discrete sliding-mode band δ_2 is calculated between the boundary $s(n) = 0^+$ and $s(n) = 0^-$. Compared to the conventional reaching law, in which the width of the discrete sliding-mode band δ_1 in (18) is a constant value, the proposed method has an adaptive width of the discrete sliding-mode band δ_2 in (25), which reduces the chattering issue. To illustrate the effectiveness of the proposed method, the sliding-mode band is shown in Figure 6. In Figure 6, the sliding surface s trajectory gradually approaches 0, x_1 and x_2 also approaches 0. It can be seen that discrete sliding-mode band δ_2 reduces to 0, rather than oscillating around the origin 0 of the conventional method in Figure 2.

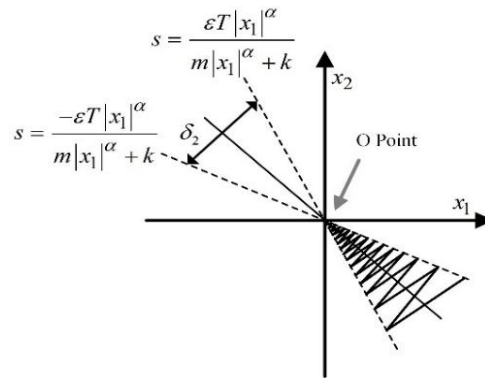$$\delta_2 = \frac{2\varepsilon T|x_1|^a}{m|x_1|^a + k} \tag{25}$$

Figure 6. State trajectory of the proposed enhanced reaching law

4.3. Stability analysis

To assess the stability of the PMSM systems, the Lyapunov stability criterion and stability analysis are employed [30]. In the Lyapunov theory, the condition for the state variables to reach the sliding surface $s = x_2 + cx_1$ is that the condition $\dot{V} < 0$ must be satisfied. In this study, we choose the Lyapunov function as a quadratic function as in (26). Taking the derivative of the (26), we obtain (27).

$$V = \frac{1}{2}s^2 \tag{26}$$

$$\dot{V} = s\dot{s} \tag{27}$$

Substituting (19) to (27), we get (28):

$$\dot{V} = s\left[-\frac{\varepsilon|x_1|^a}{m|x_1|^a + ke^{-\zeta|s|}}sgn(s) - fuzzy(q)s\right] \rightarrow$$
$$\dot{V} = -\frac{\varepsilon|x_1|^a}{m|x_1|^a + ke^{-\zeta|s|}}|s| - fuzzy(q)s^2 < 0 \tag{28}$$

where $0 < m < 1$, $\varepsilon > 0$, $m > 0$, $k > 0$, and $fuzzy(q)s^2 > 0$. The (28) guarantees the Lyapunov stability criteria $\dot{V} < 0$. Therefore, the proposed reaching law is well-suited for the PMSM motor speed control system, ensuring both stability and enhanced response.

5. EXPERIMENTAL RESULTS

To verify the effectiveness of the proposed control scheme, an experimental hardware platform for the PMSM drive system is set up. Texas Instruments microcontroller TMS280S28379D is adapted to apply the control algorithm and generate the PWM signals for controlling the PMSM motor. Figure 7 shows the experimental hardware platform, and the PMSM motor parameters are listed in Table 2. The control parameters of the conventional and proposed reaching law are listed in Table 3. For comparison, the conventional PI controller and fuzzy logic controller, which focuses on computational efficiency and real-time control, are adopted [31], [32].
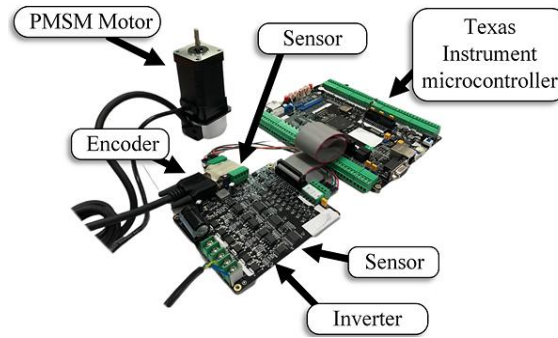
Figure 7. Experimental hardware platform for PMSM drive system

Table 2. Parameters of the PMSM motor

Symbol	Parameter	Value
p	Number of pole pairs	4
L_d, L_q	d-axis and q-axis inductance	$0.59\ mH$
R_s	Coil resistance	$1.02\ \Omega$
J	Inertia moment	$0.28\ kg.mm^2$
ψ_f	Permanent magnet flux linkage	$0.042\ Wb$
n_N	Rated speed	$3000\ rpm$
V_N	Rated voltage	$24\ Vdc$
I_N	Rated current	$4\ A$

Table 3. Parameters of the conventional and proposed reaching law

Symbol	Parameter	Conventional reaching law
N/A	Conventional reaching law	$\dot{s} = -\varepsilon\, sgn(s) - qs$
N/A	Proposed reaching law	$\dot{s} = -\dfrac{\varepsilon\|x_1\|^a}{m\|x_1\|^a + ke^{-\zeta\|s\|}} sgn(s) - fuzzy(q)s$
q	Reaching law coefficient	500
ε	Constant rate term	300
k	Error gain	0.1
a	Exponential error term	2
m	Input control gain	0.05
ζ	Error exponential coefficient	100
c	Sliding mode gain	100
K_P	Proportional gain	0.5
K_I	Integral gain	5

Figures 8(a)-8(d) illustrate the observed speed response as the PMSM speed increased from 500 rpm to 1000 rpm using a conventional PI controller, fuzzy logic controller, conventional sliding mode, and proposed sliding mode controller. The conventional PI controller ($K_P = 0.008$, $K_I = 0.0005$), as shown in Figure 8(a), had a response time of 1.1 seconds. Although the PI controller reached the desired speed, it exhibited a significant speed overshoot of 100 rpm. This level of overshoot indicates that while the PI controller can handle the speed change, it cannot completely resolve the nonlinearity effect of the PMSM motor. As seen in Figure 8(b), the fuzzy logic controller outperformed the PI controller, with a rise time of less than 0.7 seconds and a reduced speed overshoot of about 44 rpm. The faster response and smaller overshoot demonstrate the fuzzy logic controller better adaptability to the inherent nonlinearity of the PMSM motor.

In Figure 8(c), the conventional sliding mode control has a response time of 0.9 seconds, which is faster than the PI controller but slower than the fuzzy logic controller. Furthermore, the overshoot of conventional sliding mode control is smaller than that of the PI controller. Figure 8(d) shows the response of proposed sliding mode controller. The response time in Figure 8(d) was around 0.4 seconds, which is lower than PI controller fuzzy logic and also conventional sliding mode control. Also, the speed overshoot was small at only 30 rpm which is way lower than all other controllers. The results obtained reveal that the sliding mode control approach is capable of achieving high speed response with lessed overshoot in comparison of conventional techniques. To evaluate the control performance under different speed conditions, the PMSM speed reference is increased suddenly from 1000 rpm to 1500 rpm, and the results are shown in Figure 9. In Figure 9(a), the response time of the PI controller comes up to be around 1.1 seconds, which is lower compared to all other controllers, and it has a slightly higher speed overshoot of around 100 rpm. The fuzzy logic controller again performed better than the PI mode in Figure 9(b) with a response time of 0.7 seconds and an overshoot of 44 rpm. While this was faster and more stable compared to the PI controller, the overshoot still exist which may be caused by an inadequate membership function.

The response time and overshoot for the conventional sliding mode control is 0.9 s and 85 rpm shown in Figure 9(c). It is better than the PI controller but not alike to fuzzy logic and sliding mode control. As shown in Figure 9(d), the new designed sliding mode controller also had satisfactory tracking performance with a response time of only 0.4 seconds and slight overshooting speed up to about 30 rpm. Table 4 provides a comprehensive comparison between conventional PI, fuzzy logic controller, conventional sliding mode controller, and the proposed sliding mode controller. The experimental results clearly show that the proposed controller has better performance than conventional PI, fuzzy controller, and conventional sliding mode control methods in terms of response and overshoot. These results validate the proposed controller effectiveness across different speed ranges, maintaining a consistent control performance over the conventional methods. The proposed control approach provides notable advantages in regulating motor speed dynamics, surpassing the conventional technique in different speed ranges.
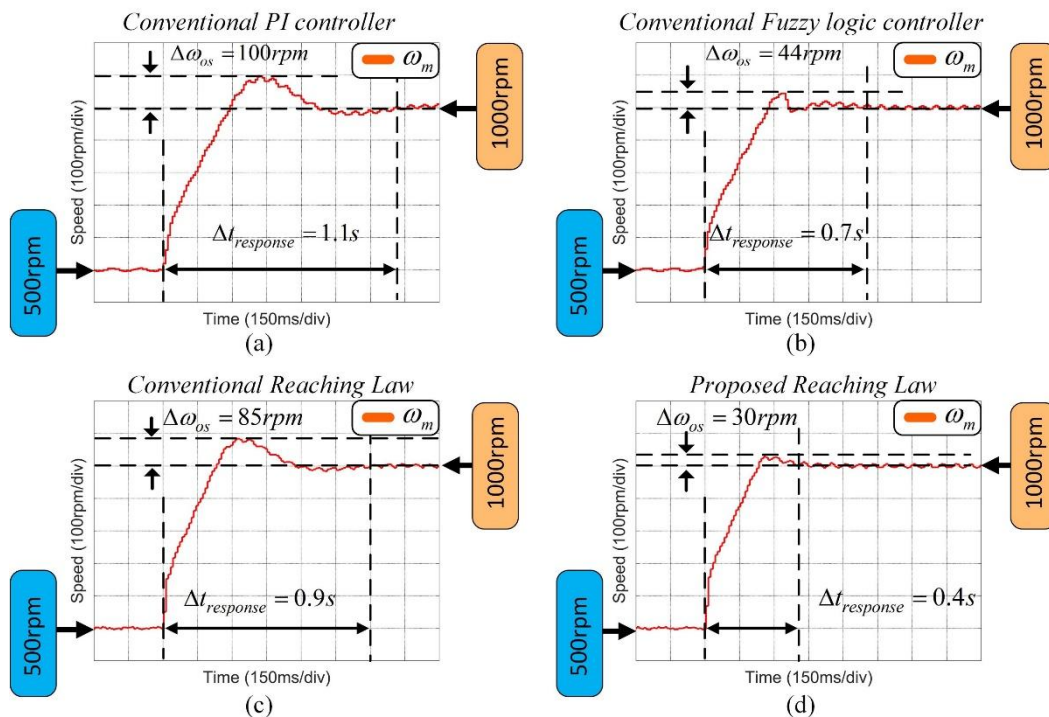

Figure 8. Experimental speed response comparison of the PI controller, fuzzy logic controller, conventional sliding mode, and proposed sliding mode controller as the PMSM speed increases from 500 rpm to 1000 rpm: (a) PI controller, (b) fuzzy logic controller, (c) conventional reaching law, and (d) proposed sliding mode controller
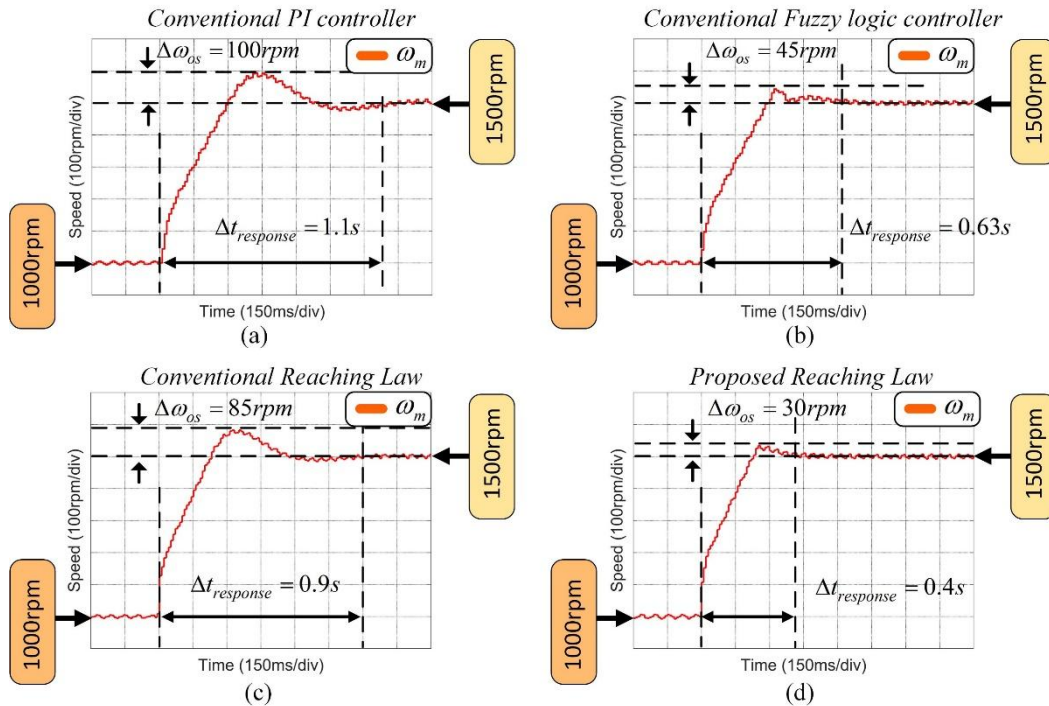
Figure 9. Experimental speed response comparison of the PI controller, fuzzy logic controller, conventional sliding mode, and proposed sliding mode controller as the PMSM speed increases from 1000 rpm to 1500 rpm: (a) PI controller, (b) fuzzy logic controller, (c) conventional reaching law, and (d) proposed sliding mode controller

Table 4. Comparison of PMSM speed control methods

Methods	Criterion				
	Complexity	Overshoot	Response	Stability	Realtime implementation in microcontroller
Conventional PI controller	Simple	High	Slow	Depend	Yes
Fuzzy logic controller	Medium	Small	Medium	Depend	Yes
Conventional sliding mode control	Medium	Medium	Medium	Good	Yes
Proposed enhanced sliding mode control	Medium	Small	High	Good	Yes

6.   CONCLUSION

This study presents an enhanced sliding mode reaching law with fuzzy logic that can simultaneously reduce the chattering effect and improve system response time. The main contributions of this paper consist in establishing a mathematical model of the PMSM and analyzing conventional reaching law limitation. Additionally, the paper presents a modified reaching law model through a fuzzy controller for better speed control performance. By adopting the proposed reaching law, the sliding gains are allowed for adjustable sliding gain, which improves the system trajectory to reach the sliding surface quickly. When the state trajectory is located near the sliding surface, the sliding gain is minimized to ensure that the state trajectory approach the sliding surface without overshoot. As a result, the integration of fuzzy and sliding mode significantly reduces the chattering, resulting in smoother and more stable motor speed control. In addition, the reachability condition ensures system stability, which is proved by Lyapunov stability theory. A small-scale PMSM experimental system has confirmed the effectiveness of this method. Also, experimental validations are conducted in various speed ranges, which further support the above results.

REFERENCES

[1] X. Sun, Z. Shi, G. Lei, Y. Guo, and J. Zhu, "Analysis and design optimization of a permanent magnet synchronous motor for a campus patrol electric vehicle," *IEEE Transactions on Vehicular Technology*, vol. 68, no. 11, pp. 10535–10544, Nov. 2019, doi: 10.1109/TVT.2019.2939794.

[2] H. Chen, A. M. El-Refaie, and N. A. O. Demerdash, "Flux-Switching Permanent Magnet Machines: A Review of Opportunities and Challenges - Part I: Fundamentals and Topologies," *IEEE Transactions on Energy Conversion*, vol. 35, no. 2, pp. 684–698, Jun. 2020, doi: 10.1109/TEC.2019.2956600.

[3] P. Ramesh, M. Umavathi, C. Bharatiraja, G. Ramanathan, and S. Athikkal, "Development of a PMSM motor field-oriented control algorithm for electrical vehicles," *Materials Today: Proceedings*, vol. 65, pp. 176–187, 2022, doi: 10.1016/j.matpr.2022.06.080.

[4] Y. Lu, Z. Jiang, C. Chen, and Y. Zhuang, "Energy efficiency optimization of field-oriented control for PMSM in all electric system," *Sustainable Energy Technologies and Assessments*, vol. 48, p. 101575, Dec. 2021, doi: 10.1016/j.seta.2021.101575.

[5] M. Zhao, Q. An, C. Chen, F. Cao, and S. Li, "Observer based improved position estimation in field-oriented controlled PMSM with Misplaced Hall-Effect Sensors," *Energies (Basel)*, vol. 15, no. 16, p. 5985, Aug. 2022, doi: 10.3390/en15165985.

[6] Q. Chen, S. Kang, L. Zeng, Q. Xiao, C. Zhou, and M. Wu, "PMSM control for electric vehicle based on fuzzy PI," *International Journal of Electric and Hybrid Vehicles*, vol. 12, no. 1, p. 75, 2020, doi: 10.1504/IJEHV.2020.104251.

[7] R. Cai, R. Zheng, M. Liu, and M. Li, "Optimal selection of PI parameters of FOC for PMSM using structured H∞-synthesis," in *IECON 2017 - 43rd Annual Conference of the IEEE Industrial Electronics Society*, IEEE, Oct. 2017, pp. 8602–8607. doi: 10.1109/IECON.2017.8217511.

[8] P. Q. Khanh and H. P. H. Anh, "Hybrid optimal fuzzy Jaya technique for advanced PMSM driving control," *Electrical Engineering*, vol. 105, no. 6, pp. 3629–3646, Dec. 2023, doi: 10.1007/s00202-023-01911-6.

[9] R. S. Widagdo, B. Hariadi, and I. A. Wardah, "Simulation of speed control on a PMSM using a PI controller," *Jambura Journal of Electrical and Electronics Engineering*, vol. 6, no. 1, pp. 63–69, Jan. 2024, doi: 10.37905/jjeee.v6i1.22287.

[10] J. M. Lazi, Z. Ibrahim, M. H. N. Talib, A. Alias, A. Nur, and M. Azri, "Speed and position estimator of for sensorless PMSM drives using adaptive controller," *International Journal of Power Electronics and Drive Systems (IJPEDS)*, vol. 10, no. 1, pp. 128–136, 2019, doi: 10.11591/ijpeds.v10.i1.pp128-136.

[11] Z. Li, W. Zhang, G. Liu, B. Wang, and Y. Zhang, "A novel integral-proportional (I-P) speed controller in PMSM motor drive," in *Proceeding of the 11th World Congress on Intelligent Control and Automation*, IEEE, Jun. 2014, pp. 4236–4241. doi: 10.1109/WCICA.2014.7053425.

[12] L. Wang, M. Tian, and Y. Gao, "Fuzzy self-adapting PID control of PMSM servo system," in *2007 IEEE International Electric Machines & Drives Conference*, IEEE, May 2007, pp. 860–863. doi: 10.1109/IEMDC.2007.382781.

[13] J.-W. Jung, V. Q. Leu, T. D. Do, E.-K. Kim, and H. H. Choi, "Adaptive PID speed control design for permanent magnet synchronous motor drives," *IEEE Transactions on Power Electronics*, vol. 30, no. 2, pp. 900–908, Feb. 2015, doi: 10.1109/TPEL.2014.2311462.

[14] C. Youssef, Z. Said, and D. Abdelkarim, "A review of non-linear control methods for permanent magnet synchronous machines (PMSMs)," in *The International Conference on Artificial Intelligence and Smart Environment*. Cham: Springer Nature Switzerland, 2024, pp. 446–452. doi: 10.1007/978-3-031-48465-0_59.

[15] Y. Chaou, S. Ziani, H. Ben Achour, and A. Daoudia, "Nonlinear control of the permanent magnet synchronous motor PMSM using Backstepping method," *WSEAS TRANSACTIONS on SYSTEMS and CONTROL*, vol. 17, pp. 56–61, Jan. 2022, doi: 10.37394/23203.2022.17.7.

[16] X. Liu, H. Yu, J. Yu, and L. Zhao, "Combined speed and current terminal sliding mode control with nonlinear disturbance observer for PMSM drive," *IEEE Access*, vol. 6, pp. 29594–29601, 2018, doi: 10.1109/ACCESS.2018.2840521.

[17] P. Mani, R. Rajan, L. Shanmugam, and Y. H. Joo, "Adaptive fractional fuzzy integral sliding mode control for PMSM model," *IEEE Transactions on Fuzzy Systems*, vol. 27, no. 8, pp. 1674–1686, Aug. 2019, doi: 10.1109/TFUZZ.2018.2886169.

[18] H. Qiu, H. Zhang, L. Min, T. Ma, and Z. Zhang, "Adaptive control method of sensorless permanent magnet synchronous motor based on super-twisting sliding mode algorithm," *Electronics (Basel)*, vol. 11, no. 19, p. 3046, Sep. 2022, doi: 10.3390/electronics11193046.

[19] J. Liu, S. Cao, Y. Yi, and Y. Fang, "Adaptive control for permanent magnet synchronous motor based on disturbance observer," in *2017 36th Chinese Control Conference (CCC)*, IEEE, Jul. 2017, pp. 3533–3537. doi: 10.23919/ChiCC.2017.8027905.

[20] X. Zhang, L. Zhang, and Y. Zhang, "Model predictive current control for PMSM drives with parameter robustness improvement," *IEEE Trans Power Electron*, vol. 34, no. 2, pp. 1645–1657, Feb. 2019, doi: 10.1109/TPEL.2018.2835835.

[21] S. Niu, Y. Luo, W. Fu, and X. Zhang, "Robust model predictive control for a three-phase PMSM motor with improved control precision," *IEEE Transactions on Industrial Electronics*, vol. 68, no. 1, pp. 838–849, Jan. 2021, doi: 10.1109/TIE.2020.3013753.

[22] Z. Wang, A. Yu, X. Li, G. Zhang, and C. Xia, "A novel current predictive control based on fuzzy algorithm for PMSM," *IEEE Journal of Emerging and Selected Topics in Power Electronics*, vol. 7, no. 2, pp. 990–1001, Jun. 2019, doi: 10.1109/JESTPE.2019.2902634.

[23] A. Wang and S. Wei, "Sliding mode control for permanent magnet synchronous motor drive based on an improved exponential reaching law," *IEEE Access*, vol. 7, pp. 146866–146875, 2019, doi: 10.1109/ACCESS.2019.2946349.

[24] Y. Wang, Y. Feng, X. Zhang, and J. Liang, "A new reaching law for antidisturbance sliding-mode control of PMSM speed regulation system," *IEEE Trans Power Electron*, vol. 35, no. 4, pp. 4117–4126, Apr. 2020, doi: 10.1109/TPEL.2019.2933613.

[25] K. M. Naikawadi, S. M. Patil, K. Kalantri, and M. R. Dhanvijay, "Comparative analysis of features of online numerical methods used for parameter estimation of PMSM," *International Journal of Power Electronics and Drive Systems (IJPEDS)*, vol. 13, no. 4, pp. 2172–2180, 2022.

[26] Mohd. Marufuzzaman, M. B. I. Reaz, and M. A. Mohd. Ali, "FPGA implementation of an intelligent current dq PI controller for FOC PMSM drive," in *2010 International Conference on Computer Applications and Industrial Electronics*, IEEE, Dec. 2010, pp. 602–605. doi: 10.1109/ICCAIE.2010.5735005.

[27] A. Kumar and D. Chatterjee, "A survey on space vector pulse width modulation technique for a two-level inverter," in *2017 National Power Electronics Conference, NPEC 2017*, vol. 2018-January, pp. 78–83, Jul. 2017, doi: 10.1109/NPEC.2017.8310438.

[28] D. Venkata Ramana, P. Chandrasekar, R. Sreedhar, K. Karunanithi, K. Aruna Rani, and A. Vijayakumar, "Performance analysis of three-phase Cuk inverter with PWM and SPWM modulation based on power quality," in *Sixth International Conference on Intelligent Computing and Applications: Proceedings of ICICA 2020*, Springer, 2021, pp. 91–99, doi: 10.1007/978-981-16-1335-7_9.

[29] R. Sreedhar, K. Karunanithi, P. Chandrasekar, and R. B. Teja, "Nearest space-vector control strategy for high-resolution multilevel inverters," in *2021 6th International Conference for Convergence in Technology (I2CT)*, IEEE, 2021, pp. 1–6, doi: 10.1109/I2CT51068.2021.9417882.

[30] Y. Li, J. Zhang, and Q. Wu, *Adaptive Sliding Mode Neural Network Control for Nonlinear Systems*. Academic Press 2018.

[31] B. Adhavan, A. Kuppuswamy, G. Jayabaskaran, and V. Jagannathan, "Field oriented control of permanent magnet synchronous motor (PMSM) using fuzzy logic controller," in *2011 IEEE Recent Advances in Intelligent Computational Systems*, IEEE, Sep. 2011, pp. 587–592. doi: 10.1109/RAICS.2011.6069379.

[32] H. Celik and T. Yigit, "Field-oriented control of the PMSM with 2-DOF PI controller tuned by using PSO," in *2018 International Conference on Artificial Intelligence and Data Processing (IDAP)*, IEEE, Sep. 2018, pp. 1–4. doi: 10.1109/IDAP.2018.8620902.

BIOGRAPHIES OF AUTHORS

Khanh Quoc Truong 🆔 📇 sc ◐ is a researcher at the Faculty of Electrical and Electronic Engineering, Ho Chi Minh City University of Technology, Vietnam. His research interests include control theory, PMSM, embedded systems, and power electronics. He can be contacted at email: khanh.truongphysci@hcmut.edu.vn.

Son Huynh 🆔 📇 sc ◐ is a researcher at the Faculty of Electrical and Electronic Engineering, Ho Chi Minh City University of Technology, Vietnam. His research interests include control theory, PMSM, embedded systems, and power electronics. He can be contacted at email: son.huynhcn123@hcmut.edu.vn.

Dung Hoang Vo 🆔 📇 sc ◐ is a researcher at the Faculty of Electrical and Electronic Engineering, Ho Chi Minh City University of Technology, Vietnam. His research interests include control theory, PMSM, embedded systems, and power electronics. He can be contacted at email: dung.vovhd03@hcmut.edu.vn.

Minh Duc Pham 🆔 📇 sc ◐ received the master and Ph.D. degrees in Electrical Engineering from Ulsan University, South Korea. He is currently a full-time lecturer at Ho Chi Minh City University of Technology, Vietnam. His research interests include hybrid AC-DC microgrids, PMSM, low-cost inverters, and renewable energy. He can be contacted at email: pmduc@hcmut.edu.vn.